10-10-1990

Measurement of the 0.3-8.5 MeV Galactic Gamma-Ray Spectrum from the Galactic Center Direction

M J. Harris
Naval Research Lab

Gerald H. Share
Naval Research Lab

Mark D. Leising
Clemson University, lmark@clemson.edu

R L. Kinzer
Naval Research Lab

D C. Messina
Naval Research Lab

THE ASTROPHYSICAL JOURNAL, 362:135–146, 1990 October 10

MEASUREMENT OF THE 0.3–8.5 MeV GALACTIC GAMMA-RAY SPECTRUM FROM THE GALACTIC CENTER DIRECTION

M. J. HARRIS,[1] G. H. SHARE, M. D. LEISING, R. L. KINZER, AND D. C. MESSINA[2]
E. O. Hulburt Center for Space Research, Naval Research Laboratory
Received 1990 January 29; accepted 1990 April 10

ABSTRACT

The low-energy γ-ray spectrum from the direction of the Galactic center has been determined from data obtained with the *Solar Maximum Mission* Gamma Ray Spectrometer between 1980 and 1987. The analysis uses a technique previously employed successfully in observations of Galactic 0.511 MeV and ^{26}Al lines. After subtracting most backgrounds due to radioactive lines and continuum in the instrument, the variation of the counts in each of the 476 channels of the spectrometer was fitted to a model which included the expected variation from plausible Galactic source distributions transiting the instrument's aperture. The spectrum was constructed from the amplitude of the increase in each channel associated with these transits.

The Galactic spectrum consists of a power-law continuum, $dN/dE \propto E^{-\alpha}$, with $\alpha = 1.5^{-0.1}_{+0.5}$ between 0.6 and 8.5 MeV (the errors include statistical and systematic uncertainties, the systematics being much the larger) upon which is superposed a line at 1.809 MeV due to ^{26}Al decay. The flux in this energy range is consistent with that expected from cosmic-ray electron bremsstrahlung. The spectrum at lower energies exhibits a strong 0.511 MeV positron annihilation line, and excess continuum below 0.511 MeV which is consistent with annihilation via positronium formation; the positronium fraction deduced is $0.89^{-0.06}_{+0.10}$ (also including both statistical and systematic errors). No other significant noninstrumental features are visible in the spectrum: a typical upper limit (at the 95% confidence level) is 2×10^{-4} photons (cm^2 s)$^{-1}$ for any line at 1 MeV.

Subject headings: galaxies: nuclei — galaxies: The Galaxy — gamma rays: general

I. INTRODUCTION

The diffuse continuum radiation emitted at MeV energies from the direction of the Galactic center has hitherto been detected only with low statistical significance or over broad energy bands (Gilman *et al.* 1978; Mandrou *et al.* 1980; O'Neill *et al.* 1983; Lavigne *et al.* 1986; an upper limit was obtained by Schönfelder, von Ballmoos, and Diehl 1988). In consequence, detailed spectra at these energies are not available. A detailed spectrum in this energy range is important because of the information it contains about radioactive isotopes, and about cosmic-ray electrons and protons at MeV and tens of MeV energies. Dispersed products of nucleosynthesis, such as ^{26}Al, are revealed by distinct narrow lines (Ramaty and Lingenfelter 1977). Other lines are expected from ambient material excited by cosmic-ray protons (Ramaty, Kozlovsky, and Lingenfelter 1979). On the other hand, the overall shape of the continuum reflects the shape of the low-energy cosmic-ray electron spectrum (Sacher and Schönfelder 1983).

At lower energies (0.3–0.511 MeV) the diffuse spectrum from the center region apparently exhibits a different continuum, due to electron-positron annihilation into three photons, related to the observed 0.511 MeV annihilation line (Lingenfelter and Ramaty 1989). The ratio of line to continuum emission, if measured with sufficient accuracy, provides an estimate of the fraction of annihilations which occur via the formation of positronium; this in turn gives information on the environment in which annihilation occurs (see § IV*a*).

In this paper we present observations of Galactic γ-rays from 0.3 to 8.5 MeV made with the Gamma Ray Spectrometer (GRS) on board the *Solar Maximum Mission* (*SMM*). The spectrum has been measured with high statistical significance and energy resolution, made possible by the accumulation of data over the eight years of the *SMM*, the large aperture of the GRS, and its exceptional gain stability. We have also performed a detailed analysis of the systematic uncertainties in our measurement. The γ-ray lines due to electron-positron annihilation and decay of ^{26}Al were observed over a power-law continuum extending to over 8 MeV; an enhanced continuum relative to this power law was observed below 0.511 MeV.

The large aperture of the GRS makes it very difficult to obtain information on the spatial distribution of the observed emission. The fact that the *SMM* has measured consistently higher 0.511 MeV line fluxes than other instruments observing the Galactic center with smaller apertures (Lingenfelter and Ramaty 1989) suggests that it is primarily observing a diffuse source rather than a central point source. In this paper we will focus upon the entire spectrum of the emission, under the general assumption that it is distributed along the Galactic plane.

The presence of a compact source at the Galactic center has been inferred from observed variations of the annihilation spectrum and the continuum around 1 MeV on time scales of the order of months (Leventhal *et al.* 1989; Riegler *et al.* 1981). Although the GRS data, as analyzed here, cannot resolve these variations either spatially or temporally, our results impact the compact source problem indirectly. The instruments making the observations had sufficiently broad apertures that some of the flux observed must have originated in the diffuse source. If the changing spectrum from the compact source is to be evaluated correctly, the underlying diffuse spectrum must be known so that it can be subtracted. In particular, when the compact source is in a state of low activity, the spectrum ought to be dominated by the residual "diffuse" emission, as presented here (see § IV*d*).

[1] S M Systems and Research Corporation, Landover, Maryland.
[2] SFA, Inc., Landover, Maryland.

II. DATA ANALYSIS

a) Instrument Operation

The GRS on the *SMM* satellite has been described in detail by Forrest *et al.* (1980). Here we summarize the salient features for the present analysis. Since 1980 February *SMM* has continuously accumulated data, except for a 5 month period (1983 November–1984 April) prior to the Space Shuttle in-orbit repair mission. Since it is permanently pointed at the Sun, the Galactic center transits the field of view of the GRS once per year, centered in December. Increases in line intensities at 0.511 and 1.809 MeV have been observed at these times (Share *et al.* 1985, 1988) and have been attributed to emission from the Galactic plane. In this paper we use the same technique on a channel-by-channel basis to obtain a spectrum of the Galactic plane.

The GRS detector comprises seven 7.6 × 7.6 cm NaI crystals whose sides and rear are surrounded by an anticoincidence shield (see the detailed description by Forrest *et al.* 1980). Its effective area is ~ 150 cm^2 at 0.511 MeV, and ~ 70 cm^2 at 1.8 MeV. It is sensitive to photon energies between 0.3 and 8.5 MeV, which are binned into 476 channels and accumulated over 16.384 s time intervals. The energy resolution is 7% at 0.62 MeV. A model of the instrument's energy response is used to test hypotheses for the incident photon spectrum against the channel-by-channel count spectrum (see § III*b*).

The angular response of the GRS is extremely broad ($\sim 130°$ FWHM at 0.511 MeV) and is energy-dependent, with the aperture increasing with photon energy. Our knowledge of the angular response is derived from Monte Carlo simulations (S. M. Matz and G. V. Jung 1988, private communication), since no preflight angular calibration was performed.

The original 16.384 s spectra are operationally summed into 1 minute accumulations, which are screened against the occurrence of a solar flare, γ-ray burst, or terrestrial background event. The 1 minute spectra are tagged with values of vertical geomagnetic cutoff rigidity, time since the last passage of the South Atlantic Anomaly (SAA), and the Sun-Earth-satellite angle. They are then summed over 3 day periods into bins defined by values of these tags (cf. Share *et al.* 1988). Our data set was compiled from the spectra available from the beginning of the mission up until 1988 September.

b) Elimination of Background

The 1 minute accumulated spectra are dominated by spectral lines and continuum arising from induced radioactive species in the spacecraft and detector (Share *et al.* 1989*a*), many of which have been identified. Very intense short-lived lines and continuum arise from bombardment of the spacecraft by energetic protons during passages of the SAA, and our first step in elimination of the background was the rejection of data from orbits during which the SAA was encountered, and from times within $\sim 10^4$ s thereafter.

The remaining spectra still contained radioactive backgrounds due to long-lived isotopes produced in the detector and spacecraft. However, these features should be present in equal intensities in spectra taken at short intervals apart, and subtracting such spectra should remove them. This procedure has been found to work when "sky-viewing" data (with the GRS pointing away from the Earth) is subtracted from the "Earth-viewing" spectra (Share *et al.* 1988).

We therefore subtracted spectra having Sun-Earth-satellite angles from 288° to 72° ("sky view") from spectra at angles from 108° to 252° ("Earth view"), after accumulating such spectra over 3 day periods. A typical resulting spectrum is shown in Figure 1. The instrumental features having largely canceled, what remains is a spectrum of the Earth's atmosphere (Letaw *et al.* 1989); any cosmic spectral features are superposed on it "in negative."

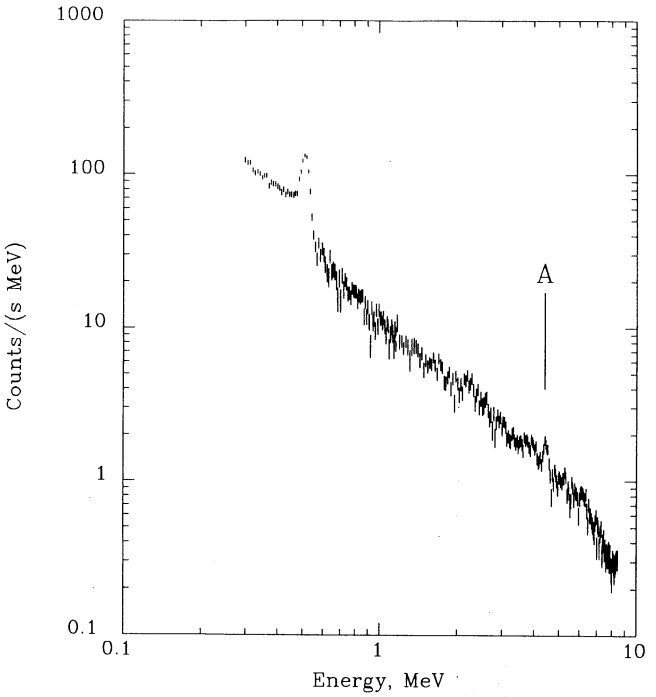

FIG. 1.—Sum of Earth-view minus sky-view spectra over 3 days (1981 January 7–10) and over all geomagnetic rigidity bins. Line feature A is produced at 4.44 MeV by cosmic-ray interactions with ^{14}N and ^{12}C in the Earth's atmosphere, and is used as an indicator of the time variation of the background from the Earth's atmosphere (see Appendix A).

We then faced the problem of separating the Galactic spectrum from the Earth's atmospheric spectrum, which was solved by exploiting the distinctive time signature expected from a cosmic source transiting the GRS aperture each year. The time series of counts in each of the 476 channels of the spectrometer was separated into a component having this "transiting" structure and a component whose time variation tracked that of radiation from the Earth's atmosphere (details are given in Appendix A). This procedure is illustrated schematically in Figure 2.

The separation of these two components was accomplished by fitting their time signatures to the time series of "Earth view minus sky view" counts in each channel. The best-fitting amplitudes for the two components, when plotted as functions of channel energy, are the two count spectra (Earth atmosphere and Galactic center).

As described in Appendix A, the precise time signature of the transiting component depends on the Galactic distribution of the source. We investigated several possible distributions, mostly derived from radio wavelength maps of CO emission, which is believed to track the distribution of mass in the inner Galaxy.

Statistical uncertainties in the spectra were determined for each channel from the quality of the fits of the time series of counts, using a standard statistical algorithm. We also expended considerable effort in evaluating the systematic errors in our analysis, which are described in Appendix B.

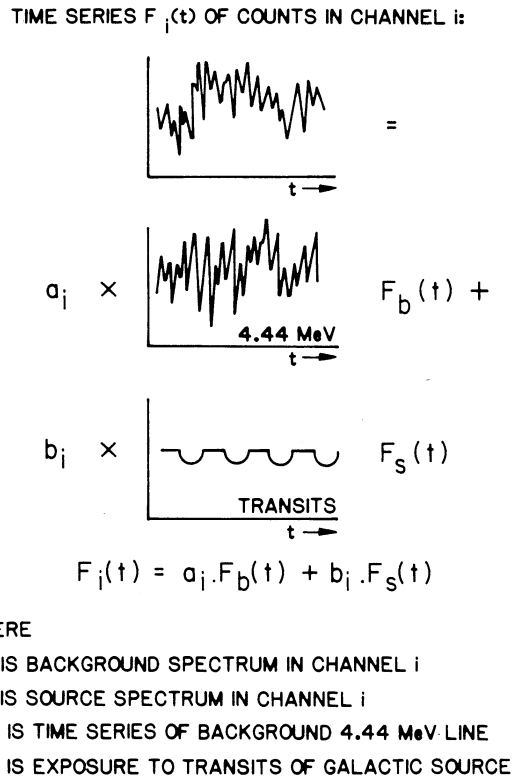

FIG. 2.—Schematic illustration of method of deriving Galactic spectrum by separating source and background time signatures in the data for one channel. Note that the Galactic (transiting) time signature is negative, as a result of the subtraction of "sky-viewing" from "Earth-viewing" data (see § II*b*).

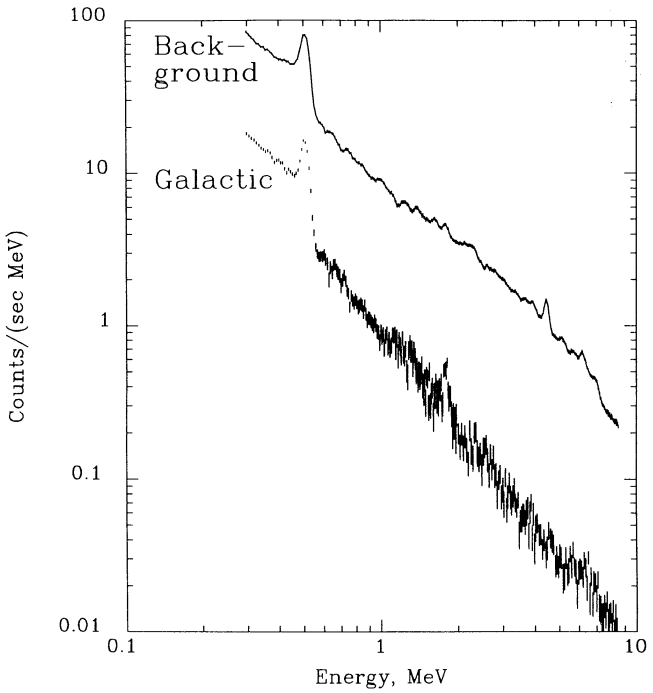

FIG. 3.—Separated spectra of the atmospheric background and the Galactic source measured by the method of separating time signatures, using 3 day spectra summed over geomagnetic rigidities above 4 GV; the CO2 distribution of Fig. 9 and the presence of a point source at the Crab Nebula position are assumed.

III. RESULTS

a) Source and Background Count Spectra

The derived spectra of the atmospheric background and the Galactic source are shown in Figure 3. The error bars are the statistical errors calculated from the quality of the fits; note that much larger systematic errors are present (see Appendix B).

The derived background spectrum is identical to the atmospheric γ-ray spectrum measured by *SMM* (Letaw *et al.* 1989). At energies below the clearly visible 0.511 MeV line, an elevated, rather flat continuum is present in the background spectrum, which is due to Compton scattering of the annihilation photons by the intervening layers of the atmosphere. Several nuclear lines are evident above a rather hard power-law continuum at higher energies.

The derived Galactic spectrum (Fig. 3) is about an order of magnitude less intense than the atmospheric background spectrum. It exhibits the expected ^{26}Al line at 1.809 MeV, superposed upon a power-law continuum above 0.511 MeV which is considerably softer than that in the atmospheric spectrum. Two weak features at 1.17 and 1.33 MeV are due to imperfect subtraction of lines from the on-board ^{60}Co radioactive calibration sources; variations in the gain of the plastic charged-particle detectors which veto positron events from these sources are probably responsible. An even weaker feature around 0.67 MeV is probably an imperfectly subtracted line arising from instrumental radioactivity (^{132}Cs arising from irradiation of the CsI anticoincidence shield, as discussed in § III of Appendix A).

We attempted to quantify the residual contamination of the Galactic spectrum by the atmospheric background by searching for any terrestrial lines in the Galactic spectrum. None of the lines were present at more than about the 2 σ level [this level corresponds to a flux $\sim 2 \times 10^{-4}$ photons (cm^2 s)$^{-1}$ for a line at 1 MeV]. We also determined that the overall atmospheric background spectral shape (lines plus continuum) above 0.511 MeV is present in the Galactic spectrum at no higher than 5% of the Galactic continuum. We conclude that the separation between the Galactic diffuse source and the terrestrial background is effectively accomplished by our analysis.

The results of our treatment of other systematic errors are discussed in § VI of Appendix B.

b) Incident Source Photon Spectrum

The Galactic spectrum plotted in Figure 3 contains five basic components: a power-law continuum which dominates above 0.511 MeV (attributed to electron bremsstrahlung), the ^{26}Al line at 1.809 MeV, the positron annihilation line at 0.511 MeV, the flat continuum between 0.3 and 0.511 MeV (usually attributed to positron annihilation via positronium), and a soft power law at very low energies (attributed to hard X-ray sources: see § II of Appendix B). The spectrum is represented as the sum of these components:

$$I(E) = A_0 E^{-\alpha_0} + A_{1.809} I_L(E) + A_{0.511} I_L(E) + A_{\rm cont} I_c(E) + A_1 E^{-\alpha_1}, \quad (1)$$

where I_c and I_L are the shapes of the 0.3–0.511 MeV continuum and of the two lines (which are assumed to be Gaussian), respectively. We derived the incident Galactic photon spectrum by constructing models of it from these components,

folding them through the instrument response function, and comparing the results with the observed count spectrum (Fig. 3). Best-fit model parameters were determined using a weighted least-squares analysis, varied to minimize the residuals.

Two different models were considered for the photon spectrum; of the five components, four were common to both models—the annihilation line, the ^{26}Al line, the high-energy power law, and the low-energy power law. The lines were assumed to have Gaussian shapes, whose widths were free parameters in the fit. The models differed in that in one case the excess continuum between 0.3 and 0.511 MeV was ascribed to positron annihilation via positronium (positronium model: $A_{\rm cont} = A_{\rm pos}$), and in the other case it was attributed to Compton scattering of the 0.511 MeV line photons in overlying material (Compton model: $A_{\rm cont} = A_{\rm Comp}$). We found for both models that the intrinsic widths of both the 0.511 MeV and ^{26}Al lines were much narrower than the nominal resolution of the GRS (~43 keV FWHM at 0.511 MeV, and ~91 keV FWHM at 1.8 MeV); in other words, they cannot be reliably determined. Note that the visual significance of the line features in the plots of our results depends on the line widths; for plotting purposes we fixed the widths of the 0.511 and 1.809 MeV lines at 3 and 1.5 keV, respectively.

Results from our "best" count spectrum (assuming the distribution model referred to as CO2 in Appendix A), using the positronium model for the spectrum, are shown in Figure 4. We list the derived parameters of the several components in Table 1. The shape of the continuum produced by annihilation from the triplet ground state of positronium into three photons is well known (see, for example, Stecker 1971). The amplitude $A_{\rm pos}$ of this component in Table 1 is the total number of photons integrated over the whole shape. The same is true of the amplitudes presented for the two Gaussian lines.

The error bars in Table 1 take into account the systematic errors discussed in Appendix B. These error bars are our estimate of the *full range* of allowed values of the parameters; they are dominated by the systematic errors, and are therefore much larger than the 1 σ statistical errors traditionally quoted.

The photon spectrum obtained using the Compton scattering model to describe the data below 0.511 MeV is almost identical with that shown for the positronium model in Figure 4; it is the interpretation of the continuum below 0.511 MeV which is different. The spectral shape produced by Compton

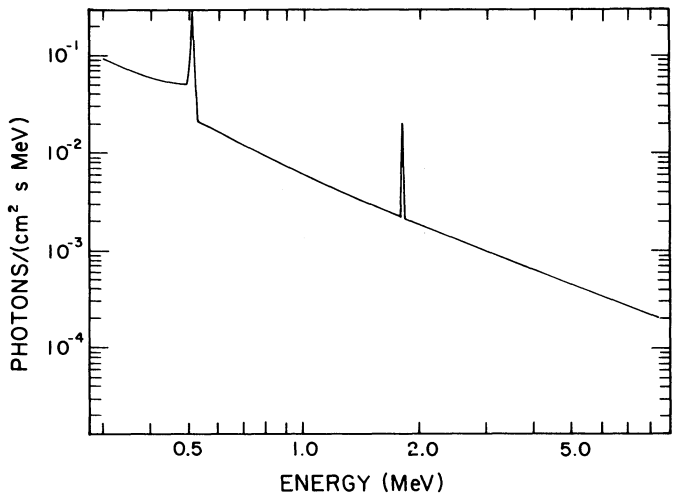

FIG. 4.—Best-fit photon spectrum of the Galactic center region measured by the method of separating time signatures, using 3 day spectra summed over all geomagnetic rigidities. The Galactic emission was assumed to be distributed according to the CO2 distribution of Fig. 9. The flux from the central radian of this distribution is plotted. Data suspected of contamination by space reactor positrons (see Appendix B) were excluded. The spectrum was described by the positronium model (see § III*b*) for the purposes of inversion of the instrument response. The line widths were not resolved and were fixed at 3 keV for the 0.511 MeV line and 1.5 keV for the 1.809 MeV line.

scattering of the 0.511 MeV line was calculated for a grid of column densities of hydrogen in the line of sight between 1 and 20 g cm^{-2}; the grammage which produced a count spectrum closest to that observed is given in Table 1. The amplitude $A_{\rm Comp}$ quoted for this shape in Table 1 is the total number of photons integrated over the energy range 0.3–0.511 MeV.

c) Spectrum from a Galactic Center Point Source Model

As noted in Appendix A, our analysis yields the results in Figure 4 and Table 1 in terms of the total flux coming from the central radian of the Galaxy. These units are suitable for comparison with theoretical calculations of the diffuse emission from the central region, and with previous measurements made by broad-aperture instruments (see § IV*c*). However, previous results have also been quoted in terms of a model in which the emission comes from a central point source (especially results for the lines: see Share *et al.* 1988 and Purcell 1989). We also

TABLE 1

DERIVED SPECTRAL PARAMETERS FOR A DISTRIBUTED GALACTIC SOURCE[a]

Component	Parameters	Positronium Model[b]	Compton Model[b]	Units
High-energy power law	A_0	$5.1^{-1.4}_{+2.4} \times 10^{-3}$	$5.7^{-1.5}_{+2.6} \times 10^{-3}$	γ (cm^2 s MeV)$^{-1}$
	α_0	$-1.52^{-0.51}_{+0.07}$	$-1.59^{-0.46}_{+0.08}$	...
^{26}Al line	$A_{1.809}$	$3.5^{-1.3}_{+0.8} \times 10^{-4}$	$3.5^{-1.3}_{+0.8} \times 10^{-4}$	γ (cm^2 s)$^{-1}$
0.511 MeV line	$A_{0.511}$	$2.3^{-0.8}_{+0.5} \times 10^{-3}$	$2.6^{-0.8}_{+0.5} \times 10^{-3}$	γ (cm^2 s)$^{-1}$
Positronium continuum	$A_{\rm pos}$	$6.7^{-2.3}_{+1.8} \times 10^{-3}$	...	γ (cm^2 s)$^{-1}$
Compton continuum	$A_{\rm Comp}$	...	$6.5 \pm 2.0 \times 10^{-3}$	γ (cm^2 s)$^{-1}$
Scattering depth	...	...	16.8 ± 2.1	g (H)
Low-energy power law	A_1	$9^{-8}_{+9} \times 10^{-4}$	$4^{-4}_{+1} \times 10^{-4}$	γ (cm^2 s MeV)$^{-1}$
	α_1	-3.26 ± 0.17	-3.0	...

[a] Expressed as the flux from the central radian of the Galactic plane.
[b] The errors represent our estimate of the *total allowed range of values.*

TABLE 2

DERIVED SPECTRAL PARAMETERS FOR A POINT SOURCE AT THE GALACTIC CENTER

Component	Parameter	Value[a]	Units
High-energy power law	A_0	$6.9^{-1.6}_{+3.1} \times 10^{-3}$	γ (cm^2 s MeV)$^{-1}$
	α_0	$-1.49^{-0.54}_{+0.04}$	...
^{26}Al line	$A_{1.809}$	$4.2^{-1.0}_{+0.9} \times 10^{-4}$	γ (cm^2 s)$^{-1}$
0.511 MeV line	$A_{0.511}$	$2.7^{-0.7}_{+0.6} \times 10^{-3}$	γ (cm^2 s)$^{-1}$
Positronium continuum	$A_{\rm pos}$	$8.0^{-1.8}_{+2.2} \times 10^{-3}$	γ (cm^2 s)$^{-1}$
Low-energy power law	A_1	$9^{-8}_{+9} \times 10^{-3}$	γ (cm^2 s MeV)$^{-1}$
	α_1	-3.30 ± 0.17	...

[a] The errors represent our estimate of the *total allowed range of values.*

calculated our results using this point-source model (§ III of Appendix B), and the results are presented in Table 2 for the purpose of comparison. For the 0.511 MeV line, our value is ~30% higher than that given by Share *et al.* but is consistent within the total uncertainties of this analysis. This discrepancy is due to several small systematic differences between the two analyses, including Share *et al.*'s use of a background correction which contained an annual modulation (see § III of Appendix A) and our improved treatment of the zero level against which transits are measured (by simultaneous fitting of Crab nebula transits: see § II of Appendix B).[3]

IV. DISCUSSION

a) Positronium Fraction

If the continuum below 0.511 MeV is interpreted as a three-photon positronium (Ps) annihilation continuum, then the fraction f of annihilations occurring through Ps formation may be calculated from the amplitudes of this continuum and of the 0.511 MeV line presented in Table 1. We express the total annihilation spectrum I in terms of the quantities in equation (1):

$$I(E) = A_{\rm pos} I_c(E) + A_{0.511} I_L(E) .$$

Of the positrons that form Ps, 75% enter the triplet ground state (orthopositronium), which decays into the three-photon continuum, while 25% enter the singlet ground state (parapositronium), which decays into two 0.511 MeV line photons. The $(1-f)$ remaining annihilations occurring "in flight" (i.e., before Ps formation) yield two 0.511 MeV photons. These fractions add up to

$$I(E) \propto 2.25 f I_c + (2 - 1.5f) I_L ,$$

so that

$$f = \frac{2}{2.25(A_{0.511}/A_{\rm pos}) + 1.5} . \quad (2)$$

We have assumed that annihilation before Ps formation occurs at low enough temperatures ($\leq 10^5$ K) that the photons are not Doppler-shifted out of the 0.511 MeV line. We also assume that orthopositronium conversion (the two-photon decay of orthopositronium under extreme conditions, as described by Brown and Leventhal 1987) is negligible, and that the lifetime of Ps against annihilation ($< 10^{-7}$ s) is so short that destruction by any other process is negligible. Applying equation (2) to our results for the line and continuum amplitudes, we obtain

$$f = 0.89^{-0.06}_{+0.10} .$$

Note that the amplitudes of the 0.511 MeV line and of the Ps continuum are correlated to some extent. Therefore, the full range of systematic error in these values in Table 1 is not reflected in the error estimate for f. Note also that according to equation (2) f is nonlinear in the line-to-continuum ratio, so that changes in the ratio produce less-than-proportionate changes in f.

Previous measurements of f in the Galactic diffuse radiation were bedeviled by the difficulty of distinguishing the Ps continuum, and by uncertainty about the possible contribution of a variable point source at the Galactic center having a different value of f, which may have been active during 1977–1979 (Lingenfelter and Ramaty 1989). Our result is consistent with most of these observations, which are characterized by values $f \sim 1$ and by large uncertainties: thus, the measurements by Johnson, Harnden, and Haymes (1972) and Johnson and Haymes (1973) have been interpreted as showing $f \sim 1.0$ (Lingenfelter and Ramaty 1989), while Leventhal, MacCallum, and Stang (1978) found $f = 0.91 \pm 0.15$, and two measurements by *HEAO 3* yielded $0.71^{-0.23}_{+0.13}$ and $1.10^{-1.10}_{+0.71}$ in 1979 fall and 1980 spring, respectively (Riegler *et al.* 1985). However, two observations in the period 1977–1979 are marginally inconsistent with our measurement ($f = 0.7^{-0.14}_{+0.12}$ obtained by Gardner *et al.* 1982 in 1977 fall, and $f = 0.5 \pm 0.15$ measured by Leventhal *et al.* 1982 in 1979 spring). It is possible that, as argued by Lingenfelter and Ramaty (1989), these low values of f together with those of Leventhal, MacCallum, and Stang (1978) and the 1979 fall *HEAO 3* measurement may be explained by a contribution from a central point source, in addition to the diffuse Galactic source which is believed to dominate the emission measured by *SMM*. If so, the true values of f measured by these experiments in the diffuse source would be larger, and therefore in better agreement with our measurement. The value of f expected from annihilation in either atomic or molecular interstellar hydrogen is very close to 0.9 (Brown 1985; Brown and Leventhal 1987).

b) A Compton Scattering Interpretation

As noted in § III*b*, an alternative interpretation of the continuum below 0.511 MeV in terms of Compton scattering is possible. Forrest (1982) pointed out that under a wide range of

[3] These two factors also contribute to the ~30% discrepancy between our result for the 0.511 MeV line flux from a distributed source (Table 1) and that of Share *et al.* (1988). In this case, another contribution to the discrepancy is due to a difference in the assumed Galactic distribution of the emission (see Appendix A; in this terminology, Share *et al.* used distribution CO3, whereas we quote our result in terms of distribution CO2). Note also that, whereas Share *et al.*'s result is given as the intensity per radian at the point $l = 0°$, $b = 0°$, ours is the value for the flux from the entire central radian of the Galactic plane.

conditions the spectral shapes produced by Ps and by Compton scattering are indistinguishable.

This scattering mechanism, although it is not forbidden by our results, is extremely difficult to justify astrophysically. As seen in Table 1, a scattering depth of ~ 17 g cm^{-2} in the line of sight is required. Such a density is orders of magnitude larger than the interstellar medium (ISM) column depth between the Sun and the Galactic center; it is more characteristic of stellar envelopes. It is, however, very difficult to imagine a steady source of positrons in stellar surface layers which is of sufficient strength and extent to explain the diffuse emission observed here. We conclude that the continuum in the region 0.3–0.511 MeV is best explained by positron annihilation through positronium formation.

c) *Cosmic-Ray Electron Continuum*

In Figure 5 we compare the photon spectrum derived from our results from Table 1 with previous broad-band measurements of the diffuse Galactic continuum. Our results agree fairly well with the other points, though our flux is somewhat higher than the general trend of the other measurements. It is also rather high compared with the line of slope -1.8 which according to Peterson *et al.* (1990) is a good representation of both the *COS B* and *HEAO 1* measurements of the unresolved flux toward the Galactic center (short-dashed line in Fig. 5).

Above 0.511 MeV and below ~ 40 MeV the diffuse γ-ray continuum is thought to be dominated by two processes involving cosmic-ray electrons: the inverse Compton effect (Compton scattering of cosmic background or starlight photons) and bremsstrahlung (Kniffen and Fichtel 1981). The theoretically expected spectra from these two processes have been discussed by Sacher and Schönfelder (1983, 1984). They arise from very different regimes of electron energy. Compton scattering of 2.7 K background photons will produce γ-rays in the ~ 1 MeV range if the electrons have energies of ~ 20 GeV; scattering of starlight (~ 500–5000 K) photons requires electron energies of ~ 1 GeV. The cosmic-ray electron energy spectrum at these GeV energies is well known in the local region of the Galaxy from direct measurements. The main uncertainty in the inverse Compton contribution to the γ-ray spectrum is due to the factor of 2 uncertainty in the energy density of starlight. Bremsstrahlung, however, produces MeV γ-rays from electrons whose energies are ~ 3 times the ensuing photon energies, i.e., in the range ~ 1–10 MeV. At these low energies the local cosmic-ray electrons are severely affected by solar modulation; although estimates from nonthermal radio emission have been made (Cummings, Stone, and Vogt 1973), the Galactic electron energy spectrum is uncertain at these energies by about two orders of magnitude. Several recipes for extrapolating from the high-energy regime down to these electron energies have been proposed; Sacher and Schönfelder (1983) present "high" (Lebrun *et al.* 1982), "medium" (Webber 1983), and "low" (Kniffen and Fichtel 1981) extrapolations. The resulting γ-ray spectra from the Galactic center direction, with the inverse Compton spectrum of Lavigne *et al.* (1986) added, are shown in Figure 6.

Our results are more compatible in magnitude with the "high" extrapolation (Fig. 6). This being the case, the electron

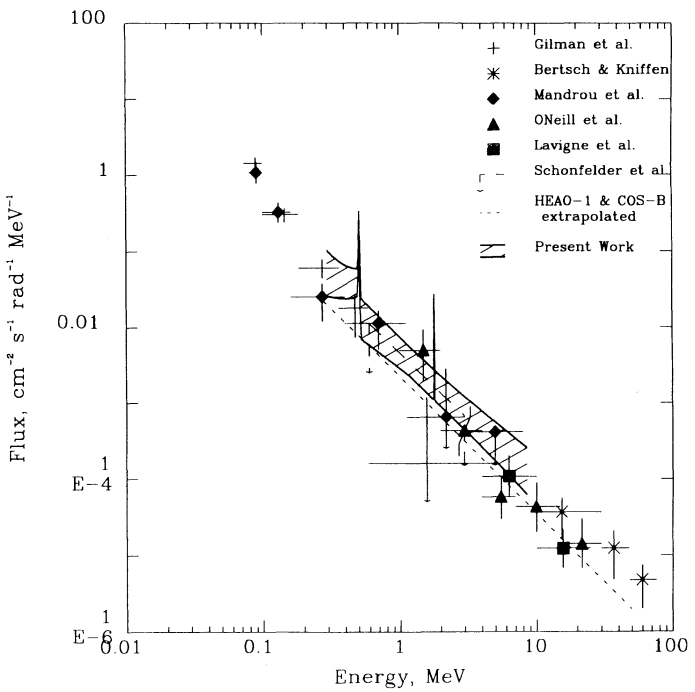

FIG. 5

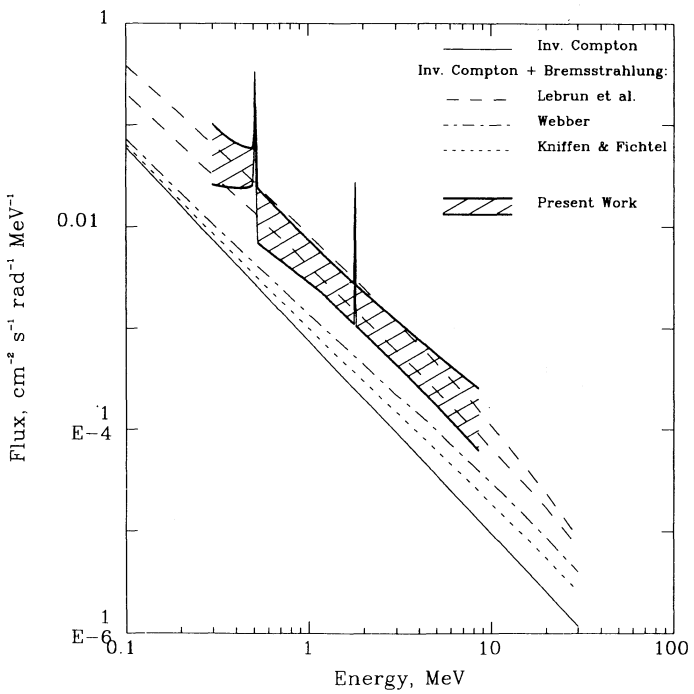

FIG. 6

FIG. 5.—Comparison of *SMM* results with previous broad-band measurements of the Galactic center region spectrum. The shaded region represents our estimate of the extreme allowed values of the spectrum, corresponding to the error bars in Table 1. The short-dashed line is Peterson *et al.*'s (1990) extrapolation upward in energy of their spectrum of the unresolved Galactic center region emission between 90 and 280 keV measured by *HEAO 1*, which is claimed to be compatible also with a downward extrapolation of the 50 MeV to 1.5 GeV *COS B* spectrum.

FIG. 6.—Comparison of *SMM* spectrum with theoretical predictions of the γ-ray continuum from the Galactic center region by Sacher and Schönfelder (1984), using three different estimates of the cosmic-ray electron energy spectrum. For the Lebrun *et al.* (1982) energy spectrum, the upper line corresponds to a cosmic-ray electron confinement time in the Galaxy of 10^7 yr and the lower line to a confinement time of 2.5×10^7 yr. For the other two energy spectra only the lower (2.5×10^7 yr) line is shown. The shaded region corresponds to the extreme range of values allowed by our results, as in Fig. 5.

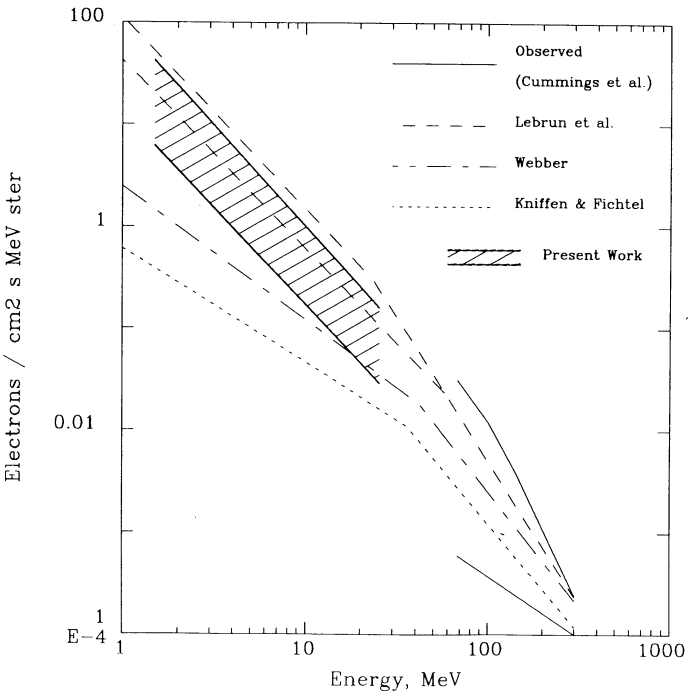

FIG. 7.—Approximate cosmic-ray electron energy spectrum deduced from the present *SMM* measurements, compared with theoretical estimates. For approximations used in deriving our spectrum see § IVc. The lines for the theoretical energy spectra are as in Fig. 6. The shaded region represents the extreme range of values allowed by our results, as in Fig. 5. The full lines are the limits on the energy spectrum measured by Cummings, Stone, and Vogt (1973).

bremsstrahlung contribution to the spectrum predominates over the inverse Compton contribution in the ~1–10 MeV energy range. We proceed to examine the implications of our results for the electron energy spectrum in this regime (Fig. 7). We derived the electron spectrum from our photon intensity spectrum by subtracting off the inverse Compton contribution (Fig. 6); if the electron energy spectrum is approximated by a power law,

$$dN_e/dE = n_0 E_e^{-\alpha} ,$$

then in the no-screening approximation the bremsstrahlung intensity,

$$I(E) = 4\sigma_0 N_H n_0 \frac{E^{-\alpha}}{\alpha - 1}\left[\ln\left(\frac{2E}{m_e c^2}\right) + \frac{1}{\alpha - 1}\right],$$

may be inverted to obtain the parameters n_0 and α (Lavigne *et al.* 1986). We assume that the column number density is $N_H = 1.5 \times 10^{22}$ atoms cm^{-2} and the bremsstrahlung cross section per atom is $\sigma_0 = 5.9 \times 10^{-28}$ cm^2. Our best power-law approximation is then

$$dN_e/dE = 38^{-26}_{+70} E^{-1.8(-0.6,+0.3)} \text{ electrons (cm}^2 \text{ s MeV sr)}^{-1} .$$

The error estimates reflect the systematic errors discussed in Appendix B, as well as the uncertainty in the inverse Compton spectrum of Figure 6. This spectrum is closest to the Lebrun *et al.* (1982) spectrum; it thus implies a "high" value for the electron flux at MeV energies. It is also somewhat flatter than the power law of index −2.3 deduced by Lavigne *et al.* (1986) from data at slightly higher energies (Fig. 5).

Strong (1985, 1988) has recently suggested that the cosmic-ray electron flux at GeV energies is about a factor of 2 higher than previously thought, arguing from the local γ-ray emissivity implied by *COS B* measurements. This effect would bring the Webber (1983) extrapolation in Figures 6 and 7 into better agreement with the Lebrun *et al.* (1982) curve (which is based directly on the *COS B* data) and with our results, especially when the uncertainty in the cosmic-ray containment time in the Galaxy is taken into account (the two dashed lines in Figs. 6 and 7 show the magnitude of this uncertainty for the Lebrun *et al.* extrapolation). The same arguments apply to the theoretical electron energy spectrum obtained by Ip and Axford (1985) from considerations of the energy-loss processes acting in the standard leaky box model (Strong 1988). Our measurements are marginally consistent with these revised Webber (1983) and Ip and Axford (1985) spectra for low values (~10^7 yr) of the cosmic-ray confinement time.

d) Galactic Center Compact Source

The presence of a point source has been postulated to account for variability in the spectrum from the Galactic center region observed by balloon and satellite experiments. An *SMM* study of the variability of the 0.511 MeV line intensity is the topic of a separate study (Share *et al.* 1990*a*). However, it is of interest to determine the contribution of the diffuse Galactic emission to the spectra associated with the reported Galactic center point source. For this reason, in Figure 8 we compare the spectrum observed by *SMM* from the Galactic center region with those observed by *HEAO 1* (Matteson 1982) and by *HEAO 3* at different times (Riegler *et al.* 1981, 1985). The *HEAO 1* spectrum and the *HEAO 3* spectrum observed in 1979 fall were reported to have been accumulated when the point source was apparently active. For the purpose of comparison

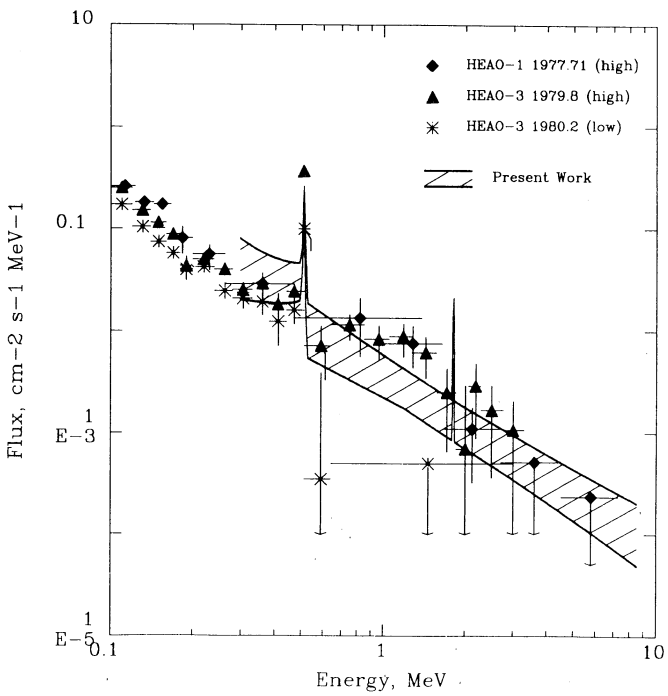

FIG. 8.—Comparison of *SMM* spectrum with those of *HEAO 3* (Riegler *et al.* 1981, 1985) and *HEAO 1* (Matteson 1982), showing the Galactic center compact 0.511 MeV line source in its "high" and "low" states. The shaded region represents the extreme range of values allowed by our results. Our results are normalized to the *HEAO 3* instrument aperture as described in § IV*d*; we neglect the small difference between the *HEAO 1* and *HEAO 3* apertures when comparing our results with those of *HEAO* 1.

we have converted the *SMM* spectrum to the equivalent spectrum from a point source which *HEAO 3* would have seen. The *SMM* spectrum plotted in Figure 5 was integrated over the *HEAO 3* aperture (Mahoney, Ling, and Jacobson 1981) to give the shaded region in Figure 8, which represents the upper and lower limits of the spectrum which *HEAO 3* would have been expected to observe from this diffuse emission. The *SMM* diffuse flux would make a slightly larger contribution to the *HEAO 1* spectrum, since the aperture of the latter experiment was slightly larger than that of *HEAO 3*, but we have neglected this difference in Figure 8.

We see that the *SMM* spectrum is in better agreement with the observations by *HEAO 1* and by *HEAO 3* in 1979 fall, when the compact central source was reportedly in a "high" or "on" state. At energies above 0.511 MeV, our spectrum lies well above the upper limits set in the 1980 spring *HEAO 3* observation, with the compact source "off." This is inconsistent with the expectation that our spectrum ought to be the residual spectrum seen by *HEAO 3* when the compact source is absent. We do not understand this discrepancy, although we note that a recent reanalysis of 0.511 MeV data from *HEAO 3* (Mahoney 1988) does not exhibit the "striking" variability between the 1979 and 1980 measurements reported earlier by Riegler *et al.* (1981, 1985).

V. CONCLUSIONS

We conclude that the diffuse γ-ray spectrum from the Galactic center region can be interpreted in a straightforward way, as the sum of the five components in equation (1), having the values in Table 1. These are the following:

1. A hard power law dominating the continuum at high energies, which is caused principally by cosmic-ray electron bremsstrahlung radiation. New constraints can be placed on the low-energy cosmic-ray electron energy spectrum as a result of this measurement (see Fig. 7).

2 and 3. Two narrow lines due to ^{26}Al decay (1.809 MeV) and positron annihilation (0.511 MeV), whose intensities agree with previous measurements.

4. An excess continuum component below 0.511 MeV, which is consistent with the annihilation of positrons through formation of Ps in a fraction $f = 0.89^{-0.06}_{+0.10}$ of cases.

5. A soft power law at low energies, which is marginally present and which is consistent with an extrapolation upward in energy of known hard X-ray sources in the Galactic center region, as described in § II of Appendix B.

We are grateful to R. Murphy and J. Letaw for their assistance, and to J. Kurfess for helpful discussions. This work was supported by NASA contract S-14513-D.

APPENDIX A

SOURCE AND BACKGROUND TIME SIGNATURES

Although the spectrum of the Galactic source is present in the spectrum of Figure 1 (as a negative component, multiplied by the exposure factor of *SMM* to the Galactic center at that time), it is clear that it cannot be extracted directly. This is true because the Galactic contribution is small relative to the spectrum from the Earth's atmosphere, and its shape is similar. We have therefore utilized the differing temporal variation patterns to separate these two spectra.

I. TIME VARIABILITY OF GALACTIC COMPONENT

The time variability which we would expect the GRS to see from a Galactic source was calculated from the known orientation of the *SMM* as a function of time. Given this, and the angular response of the GRS as a function of energy, the exposure factor to any point on the sky at any time can be computed for each channel energy. For a distributed source, the convolution of the angular response with the source distribution must be performed.

It was therefore necessary for us to assume some distribution of the Galactic emission. We investigated four distributions, three based upon maps of the CO emission at radio wavelengths and one from γ-ray data, which are shown in Figure 9. The CO maps, which trace the distribution of most of the mass in the Galactic disk, are expected as a first approximation to trace the γ-ray emission, which is also expected to be largely confined to the disk (see, e.g., Strong 1988). We have also used the divergence between different measurements of CO as an indicator of the uncertainty in the Galactic distribution of γ-rays, in our treatment of systematic errors (see § III of Appendix B).

The distributions in Figure 9 are all one-dimensional, the thickness of the plane being neglected. Distribution CO2 (the short-dashed line in Fig. 9), which was treated as the standard case, is derived from the measurements of Dame *et al.* (1987), integrated over all Galactic latitudes. The narrower distribution CO1 (solid line in Fig. 9) was obtained from the Dame *et al.* (1987) measurements integrated over Galactic latitudes $-5° \leq b \leq 5°$; the broader distribution CO3 (long-dashed line in Fig. 9) corresponds to earlier CO measurements (Burton *et al.* 1975) as fitted analytically by Leising and Clayton (1985). The *HEAO 1* distribution (plus signs in Fig. 9) was taken from the map of unresolved 90–280 keV γ-ray emission measured by *HEAO 1* (Peterson *et al.* 1990).[4] The analysis was also repeated assuming a point source at the Galactic center. Our reasons for taking the CO2 distribution to be the standard case will appear in § II of Appendix B.

The *SMM* exposure factor to the CO2 distribution, as a function of time, is shown for one channel in Figure 10. The expected peaks due to transits of the Galactic center every 12 months are plainly visible. Variations in the shape of the peak from year to year are mainly due to differences in *SMM* live time, especially the 5 month gap in 1983–1984 (around day 1500) mentioned in § II*a*. Note that the function used in fitting the time series of counts was actually the negative of the exposure function in Figure 10, due to the source spectrum appearing in negative as described above.

[4] We also considered the 50–1500 MeV γ-ray distribution found by *COS B*, as smoothed by Mahoney *et al.* (1984; not shown in Fig. 9). However, after folding with the *SMM* field of view, the GRS exposure to this distribution was so similar to that for the broad CO3 distribution of Fig. 9 that we did not investigate it further.

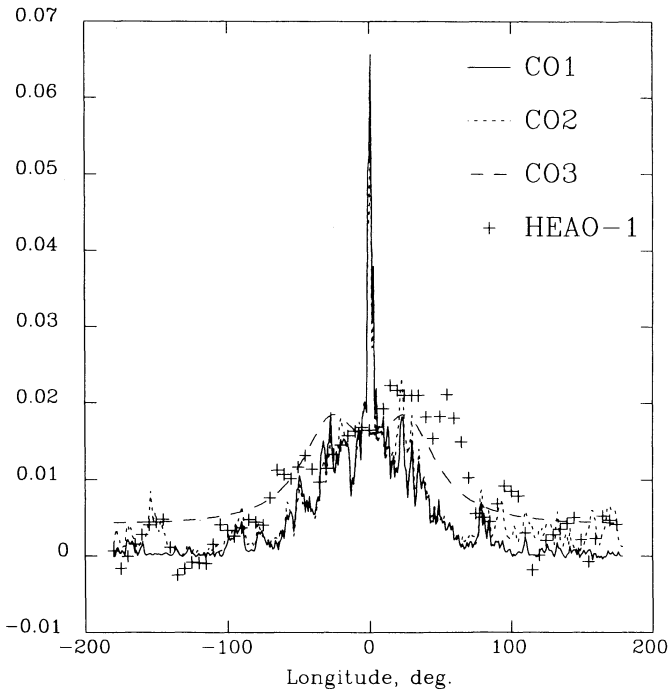

FIG. 9

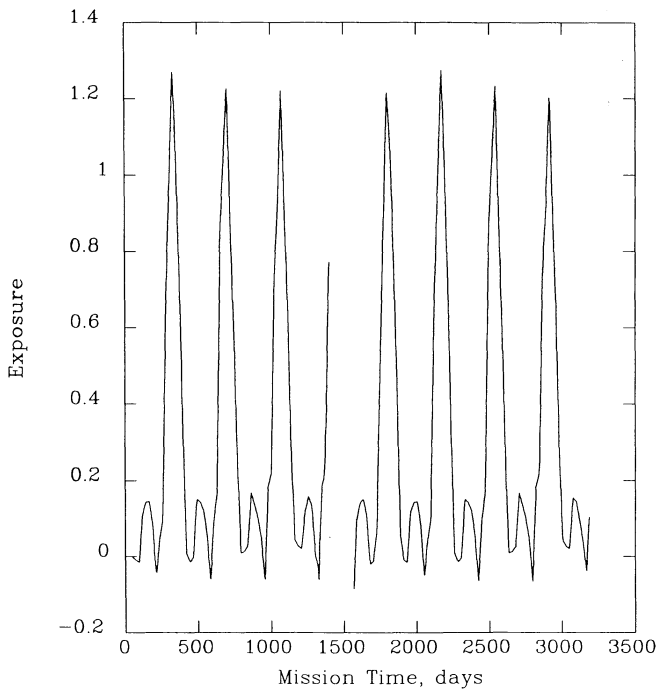

FIG. 10

FIG. 9.—Distributions of γ-ray emission with Galactic longitude used to model its transits across the *SMM* aperture. *Solid line* (CO1): the Dame *et al.* (1987) CO distribution averaged over the central 10° of latitude. *Short dashed line* (CO2): distribution of CO measured by Dame *et al.* (1987), averaged over all Galactic latitudes. *Long dashed line* (CO3): distribution of CO measured by Burton *et al.* (1975), as fitted analytically by Leising and Clayton (1985). *Plus signs*: distribution of 90–280 keV flux measured by *HEAO 1* (Peterson *et al.* 1990).

FIG. 10.—Exposure of the aperture of GRS at energy 0.510 MeV to the CO2 distribution (*dotted line*) of Fig. 9. The abscissa, "mission time," is expressed in days from 1980 January 1.

The distributions in Figure 9 are normalized to unity over the central radian of each distribution. The exposure factor in Figure 10 is therefore the expected response to the emission from the central radian of the CO2 distribution. The resulting spectrum is the number of counts from this central radian.

II. TIME VARIABILITY OF ATMOSPHERIC COMPONENT

We now discuss our method for monitoring the temporal variability of the Earth's atmospheric spectrum. We cannot simply use a template of successive spectra of the type shown in Figure 1, since each channel in that spectrum also contains some counts due to the Galactic source. It is thus important to discover some feature in this atmospheric spectrum which does not contain any Galactic component. Share *et al.* (1990*b*) have determined that the line feature at 4.44 MeV, marked "A" in Figure 1, is such a feature. It is believed to arise from de-excitation of $^{11}B^*$ (produced by spallation of ^{14}N) and of $^{12}C^*$, excited by proton impacts in the Earth's atmosphere (Letaw *et al.* 1989). Whereas the continuum above 1 MeV contains a Galactic contribution, calculations indicate that any line emission at 4.44 MeV is far below the level detectable by *SMM* (see, e.g., Higdon 1987).

The counts in this 4.44 MeV line in each 3 day spectrum were therefore fitted to a Gaussian line shape, superposed on a continuum which was assumed to be locally a power law. The variation of the integrated area under the Gaussian was taken to be the time signature of the Earth-atmosphere background, and was used to separate the atmospheric contribution to the counts observed in each energy channel (see § II*b* and Fig. 2).

III. OTHER EFFECTS HAVING A 1 YEAR PERIODICITY

In principle, if there is any effect other than transits of the Galactic center which causes background features to vary with a 1 year period, then this annual variation will be picked up along with the annual Galactic signal, giving rise to spurious features in the Galactic spectrum. An example is a line close to $\sim$670 keV, which was identified as the 0.68 MeV line from the decay of ^{132}Cs. It is believed that irradiation of the GRS's CsI anticoincidence shield during passages of the SAA produces this line. The modulation is weak, being marginally visible in Figure 7*f* of Share *et al.* (1988).

For the purposes of our present analysis, the subtraction of "sky-viewing" from "Earth-viewing" spectra, as described in § II*b*, should eliminate this 670 keV line altogether. (We found from the spectrum in Fig. 3 that this line is in fact canceled to better than 1 part in 10^3 by the subtraction.) However, we note that Share *et al.* (1988) used the same line to model the background in their measurement of the 0.511 MeV positron annihilation line (see their § IV*c*). As a result, some of the annual increase in the 0.511 MeV line intensity due to Galactic center transits in their "sky-viewing" data was attributed incorrectly to the background. Hence the Share *et al.* (1988) measurement of the intensity of the 0.511 MeV line from "sky-viewing" data is too small. A comparison of their results from "sky-viewing" data and from an "Earth minus sky view" analysis (as used in the present paper) shows that the error is about 20% (see their Table 1).

APPENDIX B

SYSTEMATIC ERRORS

Systematic errors are expected to arise in our analysis as a result of uncertainties in separating the atmospheric from the Galactic component, the presence of other sources, uncertainties in the detector response, and the choice of model used to describe the Galactic source (which will affect the time signature in Fig. 10). We took these sources of systematic error into account in our analysis, as discussed in §§ I–V of this appendix. Their impact on our results is discussed qualitatively in § VI.

I. SEPARATION OF SOURCE AND BACKGROUND

One test that we performed to determine the error due to imperfect separation was to repeat the analysis procedure on a sample of data taken at high geomagnetic cutoffs (thereby reducing the atmospheric background). We also searched for distinctive Earth-atmosphere features in the Galactic spectrum (see § III*a*).

II. EFFECTS OF OTHER CELESTIAL SOURCES

Several other sources, unrelated to the Galactic diffuse source, fall within the broad aperture of the GRS. Sources lying near the Galactic center can be separated from it only if their spectra are known to be significantly different from that of the diffuse emission, since their transits as seen by the GRS are almost identical to those of the center itself. The hard X-ray sources in the Galactic center direction have spectra which are considerably softer than the diffuse emission spectrum. The combined hard X-ray spectrum from these sources in the center direction has been measured by Leventhal, MacCallum, and Stang (1978), Leventhal *et al.* (1980), Paciesas *et al.* (1982), and Riegler *et al.* (1985). If expressed as a power law, these sources combine to produce a spectrum with a differential index (α in $dN/dE \propto E^{\alpha}$) of between about -2.3 and -2.5. We estimated the systematic error introduced by these sources by modeling the Galactic photon spectrum both with and without an additional power-law spectrum of index approximately -2.5.

A more subtle systematic error is introduced by sources in the Galactic anticenter direction over and above the emission described by the models used to fit the data. If not allowed for, they have the effect of increasing the "zero level" against which the rise in counts during a transit of the Galactic center is measured. The fitting procedure described in § II*b* returns an amplitude proportional to the difference in counts detected between the times of peak and trough in Figure 10. If some of the counts during the "trough" period come from another source, the difference (and therefore the spectrum amplitude) will be underestimated.

The Crab Nebula is the most intense source known to emit continuously at MeV energies in the anticenter direction. We therefore constructed an exposure function for a point source at the Crab's position. Since this time signature was 180° out of phase with that of Figure 10, we were able to obtain acceptable fits to its amplitudes for each of the spectral channels, in just the same way as we did with the Galactic source. In other words, the time series of counts in each energy channel was fitted with the sum of three time signatures (the 4.44 MeV background line, the Galactic source signature of Fig. 10, and a Crab Nebula transiting signature).

Having obtained a count spectrum of the Crab Nebula in this fashion, we derived a photon spectrum by assuming that it followed a single power law and deriving the best-fit parameters, after passing trial spectra through the instrument response and comparing the results with the count spectrum. Our photon spectrum was in good agreement with previous measured spectra in this energy range, and with extrapolations upward in energy from Jung's (1989) results and downward from those of *COS B* (Clear *et al.* 1987).

Just as this Crab emission affects the spectrum derived for the Galactic center region, so the form assumed for the distribution of the Galactic emission far from the center (Fig. 9) has a strong impact on the spectrum measured from the Crab. This impact is particularly pronounced at the 0.511 MeV line. Transits of any diffuse emission in the anticenter direction cannot be separated from those of the Crab; therefore, if the assumed Galactic 0.511 MeV line distribution is too broad, it takes a share of the counts which ought to appear in the Crab spectrum. A "negative" 0.511 MeV line then appears in the Crab spectrum. Conversely, a spurious 0.511 MeV line is produced in the Crab spectrum if the assumed Galactic distribution is too narrow. Under the assumption that there is no intrinsic 0.511 MeV line present in the Crab spectrum, we found that the CO2 distribution (Fig. 9) produced the best fit. Strictly speaking, this conclusion is only valid for the positron annihilation components of our spectrum, but we assume in §§ III and IV that the whole diffuse Galactic spectrum obeys this CO2 distribution. (We took into account the effect of varying the distribution, as described in the next section, as a source of systematic error.)

We estimated the systematic uncertainty in the Galactic center spectrum due to the presence of the Crab by taking two "extreme" values of the Crab spectrum and performing the separation of the three time signatures with the Crab term forced to these values in each channel. The Crab spectra we used for this purpose were extrapolations upward in energy of the recent measurements at a few hundred keV by Sunyaev *et al.* (1988) and by Jung (1989), represented by power laws with indices -2.16 and -2.56, respectively.

Two other sources which might in principle affect the Galactic spectrum are Centaurus A and Cygnus X-1. These sources are both known to vary with time at X-ray energies, and episodic emission at MeV energies has been reported from them (Ling 1988; von Ballmoos, Diehl, and Schönfelder 1987). We estimated the possible effect of these sources conservatively, by forcing the contribution from them in each channel to be that during their high-emission states. These extreme spectra were those observed by Ling *et al.* (1987) and McConnell *et al.* (1989) for Cyg X-1 and by von Ballmoos, Diehl, and Schönfelder (1987) for Cen A. These fixed spectra were modulated by transiting time signatures appropriate to sources at $l = 309°$ (for Cen A) and $l = 71°$ (for Cyg X-1) and included in the fit, in just the same way as the Crab spectrum was.

Finally, we note that, because of its large field of view, the spectrometer is exposed to a substantial isotropic flux of photons from the cosmic diffuse background. Because of the modest shielding of the *SMM* spectrometer, the subtraction of sky-viewing from Earth-viewing data (§ II*b*) causes partial, but not total, cancellation of this flux. We therefore determined the instrument's exposure to this background as a function of time. The systematic error in the Galactic center spectrum due to the presence of this

background was estimated in the same way as for Cen A and Cyg X-1; our analysis was performed both with and without an additional time signature corresponding to the diffuse background exposure, the amplitude of which in each channel was forced to the previously known spectrum, i.e., in this case the diffuse background spectrum estimated by Kinzer, Johnson, and Kurfess (1978) from a variety of measurements.

III. SPATIAL DISTRIBUTION OF THE EMISSION

The third class of systematic errors arises from uncertainties in the spatial distribution of the Galactic emission. Convolving various assumed distributions with the instrument's angular response leads to uncertainties in the shape and height of the derived transit function in Figure 10. We estimated the uncertainty by repeating the analysis for the different distributions shown in Figure 9. In addition to the standard CO2 distribution, CO distributions both narrower in longitude (CO1) and broader in longitude (CO3), the *HEAO 1* distribution, and also a central point source were considered.

IV. POSITRONS FROM NUCLEAR-POWERED SATELLITES

Contamination of the 0.511 MeV line by annihilation of positrons from space-borne nuclear reactors (Share *et al.* 1989*b*) was estimated by comparing results when the problem was severe and when it was insignificant. The less significant contamination came from reactors in 260 km orbits, and was handled by excluding data taken at times when transient annihilation events were detected. When reactors in 790 km orbits were in operation, contamination of the data was much more severe. All data from these periods (effectively, from 1987 March 1 to the end of the data set in 1988 September) were excluded from our analysis. The effects of including or excluding the contaminated data were evaluated.

V. THE DETECTOR RESPONSE FUNCTION

We investigated two possible uncertainties arising from imperfect knowledge of the instrument response. One such uncertainty arises from limited knowledge of the energy dependence of the GRS's angular response. This leads to uncertainties in the energy dependence of the transit function in Figure 10. We estimated the magnitude of the uncertainty by performing the analysis with the energy dependence suppressed, i.e., assuming the same (mean) angular response at all energies.

There is also a degree of uncertainty in the rejection of Compton-degraded γ-ray photons by the instrument's anticoincidence shield. We used the 0.511 MeV events arising from reactor positrons (see § IV of this appendix) to estimate this effect. These events were assumed to be incident on the NaI detector as a pure 0.511 MeV beam. As noted by Rieger *et al.* (1989), the observed count spectrum contains an excess at energies below 0.511 MeV in comparison with what is estimated when this line is convolved with the adopted GRS response function (see their Fig. 1*B*). We conservatively interpret this excess as being entirely due to Compton degradation of 0.511 MeV photons in the detector. To estimate the resulting uncertainty, we altered the instrument response function to enhance the response below the photopeak to agree with the reactor data. We then determined the photon spectrum from our best count spectrum as described in § III*b* using this modified instrument response.

VI. RESULTS

Here we discuss the effects of the above systematic uncertainties upon parameters of the five components of the Galactic diffuse spectrum (eq. [1]).

As discussed in § III*a*, contamination of the Galactic spectrum by background emission from the Earth's atmosphere (see § I of this appendix) is at most a few percent. The uncertainty in our measurement of the 0.511 MeV line intensity arises mainly from this contamination. When the positronium fraction f is calculated from our measurements of this line and the positronium continuum (see § IV*a*), this source of uncertainty (in the continuum) is the major contributor to the lower error bound.

The spectra of the Crab Nebula and the hard X-ray sources toward the Galactic center (§ II of this appendix) are much steeper than the Galactic continuum, so they primarily affect the Galactic results at energies below ~ 1 MeV. Uncertainties in the true spectral index of the Crab emission, and in the intensity of the hard X-ray sources, contributed most of the uncertainty in the upward direction in our derived value of the positronium fraction f (see § IV*a*).

The "high-state" spectra of Cen A and Cyg X-1 (see § II of this appendix) are relatively more intense at energies above 1 MeV. We found that Cen A had a negligible effect on the Galactic spectrum. Cyg X-1, however, whose "high-state" spectrum has a pronounced bump at 1 MeV (Ling *et al.* 1987) and strong, approximately power-law emission above 2 MeV (McConnell *et al.* 1989), affected the Galactic spectrum considerably. Since it is close enough to the Galactic center that counts which would otherwise be attributed to the transiting Galactic source were then attributed to Cyg X-1, its inclusion brings down the Galactic spectrum at energies above ~ 1 MeV. This is by far the largest source of systematic error (about a factor of 2, varying with energy, in the downward direction) in the high-energy power-law component of the spectrum.

The cosmic diffuse background emission (see § II of this appendix) also has a harder spectrum than the Crab, so that its effects on the Galactic spectrum were seen in all five components of the latter. These effects, however, were found to be small. They may be summarized as producing an increase in the amplitude of each Galactic component of $\sim 20\%$ or less when the diffuse background emission was assumed to be present having the composite spectrum given by Kinzer, Johnson, and Kurfess (1978).

The changes in the shape of the transit function in Figure 10 due to the possible Galactic distributions shown in Figure 9 (see § III of this appendix) produced small errors ($\sim 10\%$) in the Galactic spectrum. However, if the distribution was assumed to be a point source at the Galactic center, the derived Galactic flux increased by $\sim 25\%$ (compare Tables 1 and 2). These systematic errors affected all components of the spectrum equally.

Of the detector-related errors discussed in the preceding section, the uncertainty in the angular response of the GRS was found to be a small source of systematic error ($\leq 10\%$). The possible underestimate of the detector's rejection of Compton-degraded photons had the effect of producing an overestimate of the contribution from the continuum. When this is taken into account, the incident

continuum should be reduced. Therefore, a smaller incident photon amplitude was necessary to explain the observed counts. The magnitudes of the two power-law components in equation (1) were therefore reduced by ~25% as a result of this effect. The positronium continuum component was virtually unaffected, because the reduction in the amplitudes of the two power laws was sufficient to achieve the necessary reduction of the flux in the 0.3–0.511 MeV region.

The effects of the remaining errors discussed above were found to be small. Limiting the sample of data to those accumulated only at high geomagnetic rigidities (i.e., low cosmic-ray backgrounds; see § I of this appendix) or deleting over a year of data when high-altitude space reactors were aloft (§ IV of this appendix) had the effect of worsening the statistical quality of the fits, without significantly changing the parameters of the various components of the Galactic spectrum.

REFERENCES

Bertsch, D. L., and Kniffen, D. A. 1983, *Ap. J.*, **270**, 305.
Brown, B. L. 1985, *Ap. J. (Letters)*, **292**, L67.
Brown, B. L., and Leventhal, M. 1987, *Ap. J.*, **319**, 637.
Burton, W. B., Gordon, M. A., Bania, T. A., and Lockman, F. J. 1975, *Ap. J.*, **202**, 30.
Clear, J., Bennett, K., Buccheri, R., Grenier, L. A., Hermsen, W., Mayer-Hasselwander, H. A., and Sacco, B. 1987, *Astr. Ap.*, **174**, 85.
Cummings, A. C., Stone, E. C., and Vogt, R. E. 1973, *Proc. 13th Internat. Cosmic Ray Conf.*, **1**, 335.
Dame, T. M., *et al.* 1987, *Ap. J.*, **322**, 706.
Forrest, D. J. 1982, in *The Galactic Center*, ed. G. R. Riegler and R. D. Blandford (New York: AIP), p. 160.
Forrest, D. J., *et al.* 1980, *Solar Phys.*, **65**, 15.
Gardner, B. M., Forrest, D. J., Dunphy, P. P., and Chupp, E. L. 1982, in *The Galactic Center*, ed. G. R. Riegler and R. D. Blandford (New York: AIP), p. 144.
Gilman, D., Metzger, A. E., Parker, R. H., and Trombka, J. I. 1978, in *Gamma Ray Spectroscopy in Astrophysics*, ed. T. L. Cline and R. Ramaty (NASA TM 76619), p. 190.
Higdon, J. C. 1987, *Proc. 20th Internat. Cosmic Ray Conf.*, **1**, 160.
Ip, W.-H., and Axford, W. I. 1985, *Astr. Ap.*, **149**, 7.
Johnson, W. N., Harnden, F. R., and Haymes, R. C. 1972, *Ap. J. (Letters)*, **172**, L1.
Johnson, W. N., and Haymes, R. C. 1973, *Ap. J.*, **184**, 103.
Jung, G. V. 1989, *Ap. J.*, **338**, 972.
Kinzer, R. L., Johnson, W. N., and Kurfess, J. D. 1978, *Ap. J.*, **222**, 370.
Kniffen, D. A., and Fichtel, C. E. 1981, *Ap. J.*, **250**, 389.
Lavigne, J. M., Mandrou, P., Niel, M., Agrinier, B., Bonfand, E., and Parlier, B. 1986, *Ap. J.*, **308**, 370.
Lebrun, F., *et al.* 1982, *Astr. Ap.*, **107**, 390.
Leising, M. D., and Clayton, D. D. 1985, *Ap. J.*, **294**, 591.
Letaw, J. R., Share, G. H., Kinzer, R. L., Silberberg, R., Chupp, E. L., Forrest, D. J., and Rieger, E. 1989, *J. Geophys. Res.*, **94**, 1211.
Leventhal, M., MacCallum, C. J., Barthelmy, S. D., Gehrels, N., Teegarden, B. J., and Tueller, J. 1989, *Nature*, **339**, 36.
Leventhal, M., MacCallum. C. J., Huters, A. F., and Stang, P. D. 1980, *Ap. J.*, **240**, 338.
———. 1982, *Ap. J. (Letters)*, **260**, L1.
Leventhal, M., MacCallum, C. J., and Stang, P. D. 1978, *Ap. J. (Letters)*, **225**, L11.
Ling, J. C. 1988, in *Nuclear Spectroscopy of Astrophysical Sources*, ed. N. Gehrels and G. H. Share (New York: AIP), p. 315.
Ling, J. C., Mahoney, W. A., Wheaton, W. A., and Jacobson, A. S. 1987, *Ap. J. (Letters)*, **321**, L117.
Lingenfelter, R. E., and Ramaty, R. 1989, *Ap. J.*, **343**, 686.
Mahoney, W. A. 1988, in *Nuclear Spectroscopy of Astrophysical Sources*, ed. N. Gehrels and G. H. Share (New York: AIP), p. 149.
Mahoney, W. A., Ling, J. C., and Jacobson, A. S. 1981, *J. Geophys. Res.*, **86**, 11098.
Mahoney, W. A., Ling, J. C., Wheaton, W. A., and Jacobson, A. S. 1984, *Ap. J.*, **286**, 578.
Mandrou, P., Bui-Van, A., Vedrenne, G., and Niel, M. 1980, *Ap. J.*, **237**, 424.
Matteson, J. L. 1982, in *The Galactic Center*, ed. G. R. Riegler and R. D. Blandford (New York: AIP), p. 109.
McConnell, M. L., Forrest, D. J., Owens, A., Dunphy, P. P., Vestrand, W. T., and Chupp, E. L. 1989, *Ap. J.*, **343**, 317.
O'Neill, T., Dayton, B., Long, J., Zancresso, E., Zych, A., and White, R. S. 1983, *Proc. 18th Internat. Cosmic Ray Conf.*, **9**, 45.
Paciesas, W. S., Cline, T. L., Teegarden, B. J., Tueller, J., Durouchoux, P., and Hameury, J. M. 1982, *Ap. J. (Letters)*, **260**, L7.
Peterson, L. E., Gruber, D. E., Jung, G. V., and Matteson, J. L. 1990, *Proc. 21st Internat. Cosmic Ray Conf.* (Adelaide), OG 1.2-7.
Purcell, W. R. 1989, Ph.D. thesis, Northwestern University.
Ramaty, R., Kozlovsky, B., and Lingenfelter, R. E. 1979, *Ap. J. Suppl.*, **40**, 487.
Ramaty, R., and Lingenfelter, R. E. 1977, *Ap. J. (Letters)*, **213**, L5.
Rieger, E., Vestrand, W. T., Forrest, D. J., Chupp, E. L., Kanbach, G., and Reppin, C. 1989, *Science*, **244**, 441.
Riegler, G. R., Ling, J. C., Mahoney, W. A., Wheaton, W. A., and Jacobson, A. S. 1985, *Ap. J. (Letters)*, **294**, L13.
Riegler, G. R., Ling, J. C., Mahoney, W. A., Wheaton, W. A., Willett, J. B., Jacobson, A. S., and Prince, T. A. 1981, *Ap. J. (Letters)*, **248**, L13.
Sacher, W., and Schönfelder, V. 1983, *Space Sci. Rev.*, **36**, 249.
———. 1984, *Ap. J.*, **279**, 817.
Schönfelder, V., von Ballmoos, P., and Diehl, R. 1988, *Ap. J.*, **335**, 748.
Share, G. H., Kinzer, R. L., Kurfess, J. D., Forrest, D. J., Chupp, E. L., and Rieger, E. 1985, *Ap. J. (Letters)*, **292**, 221.
Share, G. H., Kinzer, R. L., Kurfess, J. D., Messina, D. C., Purcell, W. R., Chupp, E. L., Forrest, D. J., and Reppin, C. 1988, *Ap. J.*, **326**, 717.
Share, G. H., Kinzer, R. L., Strickman, M. S., Letaw, J. R., Chupp, E. L., Forrest, D. J., and Rieger, E. 1989*a*, in *High-Energy Radiation Background in Space*, ed. A. C. Rester, Jr., and J. I. Trombka (New York: AIP), p. 266.
Share, G. H., Kurfess, J. D., Marlow, K. W., and Messina, D. C. 1989*b*, *Science*, **244**, 444.
Share, G. H., Leising, M. D., Messina, D. C., and Purcell, W. R. 1990*a*, *Ap. J. (Letters)*, **358**, L45.
Share, G. H., Messina, D. C., Leising, M. D., and Kinzer, R. L. 1990*b*, in preparation.
Stecker, F. W. 1971, *Cosmic Gamma Rays* (Washington, DC: NASA).
Strong, A. W. 1985, *Proc. 19th Internat. Cosmic Ray Conf.*, **1**, 333.
———. 1988, in *Gamma-Ray Astronomy with COMPTEL in Perspective*, ed. V. Schönfelder (Garching: MPE), p. 94.
Sunyaev, R. A., *et al.* 1988, *Soviet Astr. Letters*, **14**, 247.
von Ballmoos, P., Diehl, R., and Schönfelder, V. 1987, *Ap. J.*, **312**, 134.
Webber, W. R. 1983, in *Composition and Origin of Cosmic Rays*, ed. M. M. Shapiro (Dordrecht: Reidel), p. 83.

MICHAEL J. HARRIS: S M Systems and Research Corporation, Suite 510, 8401 Corporate Drive, Landover, MD 20785

ROBERT L. KINZER, MARK D. LEISING, and GERALD H. SHARE: Mail Code 4150, Naval Research Laboratory, Washington, DC 20375-5000

DANIEL C. MESSINA: SFA, Incorporated, 1401 McCormick Drive, Landover, MD 20785